Optical properties and energy transfer processes in (Tm 3 + , Nd 3 +) doped tungstate fluorophosphate glass

Marconi J. S. Brandão, Cid B. de Araújo, Gael Poirier, Younes Messaddeq, and M. Poulain

Optical properties and energy transfer processes in (Tm^{3+}, Nd^{3+}) doped tungstate fluorophosphate glass

Marconi J. S. Brandão and Cid B. de Araújo[a]
Departamento de Física, Universidade Federal de Pernambuco, 50670-901 Recife, Pernambuco, Brazil

Gael Poirier and Younes Messaddeq
Instituto de Química, Universidade Estadual Paulista, 14801-970, Araraquara, Sao Paolo, Brazil

M. Poulain
Laboratoire des Matériaux Photoniques, Bat 10B, Campus de Beaulieu, Université de Rennes I, Rennes, France

We investigate the linear optical properties and energy transfer processes in tungstate fluorophosphate glass doped with thulium (Tm^{3+}) and neodymium (Nd^{3+}) ions. The linear absorption spectra from 370 to 3000 nm were obtained. Transitions probabilities, radiative lifetimes, and transition branching ratios were determined using the Judd-Ofelt [Phys. Rev. **127**, 750 (1962); J. Chem. Phys. **37**, 511 (1962)] theory. Frequency up-conversion to the blue region and fluorescence in the infrared were observed upon pulsed excitation in the range of 630–700 nm. The excitation spectra of the luminescence were obtained to understand the origin of the signals. The temporal decay of the fluorescence was measured for different concentrations of the doping ions. Energy transfer rates among the Tm^{3+} and Nd^{3+} ions were also determined. © *2006 American Institute of Physics.* [DOI: 10.1063/1.2200737]

I. INTRODUCTION

Energy transfer (ET) processes among rare-earth (RE) ions are important in solid state systems because they can favor luminescence emission and therefore the reduction of laser threshold or enhancement of amplifiers gain can be obtained. This is usually exploited by the introduction of donor ions into the host material in addition to the acceptor ions, which are responsible for the luminescence of interest. The donor ions are excited by the incident light source and transfer all or fraction of the absorbed energy to the acceptors.

Large band gap crystals and special glasses doped with RE ions are frequently investigated for uses in lasers, optical amplifiers, and frequency converters with basis on ET mechanisms. In particular, thulium (Tm^{3+}) and neodymium (Nd^{3+}) ions are recognized as efficient RE ions for obtaining laser emission and frequency up-conversion (UC).[1,2] A large number of reports are available where detailed spectroscopic properties of Tm^{3+} and Nd^{3+} were analyzed in glasses such as fluorozirconate,[1–4] fluoroindate,[5–8] fluorophosphate,[9,10] and silicate.[1,2,11] The investigation of ET processes between Tm^{3+} and Nd^{3+} was reported for different host materials.[12,13] Each host presents certain characteristics that favor specific applications. For example, fluorophosphate glasses have been investigated because of their potential as laser materials and optical amplifier media.[9,14,15]

Here we present results for tungstate fluorophosphate (TFP) glass that is a new emerging photonic material. Recently, TFP glasses have been considered as host materials for fluorescence studies of RE ions and for nonlinear optics.

In Ref. 16 physical properties of TFP were investigated with respect to their chemical composition. Density, refractive index, and characteristic temperatures were measured. Structural characterizations were performed by x-ray absorption near edge structure (XANES) at the tungsten L_I and L_{III} absorption edges and by Raman spectroscopy. These studies allowed the conclusion that the vitreous network is formed by WO$_6$ octahedrons. It was observed the break in the linear phosphate chains, the formation of P–O–W bonds and the presence of W–O–W bonds when the WO$_3$ concentration is larger than 30% molar, due to formation of WO$_6$ clusters. Raman spectroscopy indicates that the energy of the cutoff phonons is $\approx$930 cm^{-1}. Spectroscopic properties of Tm^{3+} doped TFP were reported in Ref. 17. Transitions probabilities, branching ratios, and radiative lifetimes associated to the Tm^{3+} states were determined. Frequency up-conversion processes and a characterization of multiphonon relaxation in TFP were also reported. The optical nonlinearity of TFP was studied in the visible and in the infrared[18,19] and their performance for optical limiting applications was controlled adjusting the WO$_3$ concentration.

In the present paper we study optical properties and ET processes in (Tm^{3+} and Nd^{3+}) doped TFP. Linear optical absorption spectroscopy was used to determine the transition probabilities, branching ratios, and radiative lifetimes of Nd^{3+} levels. The samples were excited with pulsed lasers operating in the visible range and ET between Tm^{3+} and Nd^{3+} were investigated. UC emission in the blue region and fluorescence in the infrared were observed and the mechanisms contributing for the emissions were clarified. The study of the dynamics of the fluorescence signals allowed the determination of ET rates between Tm^{3+} and Nd^{3+} ions.

---

[a]Author to whom correspondence should be addressed. Electronic mail: cid@df.ufpe.br

TABLE I. Chemical compositions of the samples (in mol %).

Sample	NaPO$_3$	BaF$_2$	WO$_3$	TmF$_3$	NdF$_3$
NBW(0.2Tm)	47.8	12	40	0.2	⋯
NBW(1Tm)	47.0	12	40	1.0	⋯
NBW(1Nd)	47.0	12	40	⋯	1.0
NBW(0.2Tm;0.5Nd)	47.3	12	40	0.2	0.5
NBW(0.2Tm;0.75Nd)	47.05	12	40	0.2	0.75
NBW(0.2Tm;1Nd)	46.8	12	40	0.2	1.0

II. EXPERIMENTAL DETAILS

The glass samples studied have the following starting compositions in mol %: (48-x-y) NaPO$_3$-12 BaF$_2$-40 WO$_3$-x TmF$_3$-y NdF$_3$, where x=0, 0.2, and 1.0; y=0, 0.5, 0.75, and 1.0. TmF$_3$ and NdF$_3$ were synthesized by fluoration of Tm$_2$O$_3$ and Nd$_2$O$_3$. Each oxide was mixed with ammonium bifluoride (NH$_4$F, HF), heated at 300 °C for fluoration and then at 500 °C for evaporation of the excess of ammonium bifluoride. All components were mixed and melted in air atmosphere at 1000 °C for 1 h in a platinum crucible. The melt was then casted in a mold preheated near the transition temperature (415 °C) and treated at this temperature for 2 h in order to remove mechanical stress upon cooling. Samples with typical dimensions of $0.5 \times 1.0 \times 0.2$ cm^3 and good optical quality were obtained.

Absorption spectra were obtained using a double-beam commercial spectrophotometer operating from 370 to 3000 nm. The dynamic of the excited states was studied using a dye laser pumped by the second harmonic of a Nd:YAG (yttrium aluminum garnet) laser, which produces 8 ns pulses with a repetition rate of 5 Hz operating from 630 to 700 nm.

The fluorescence emissions were dispersed using a 0.50 m spectrometer, with a resolution of 5 Å, coupled to a photomultiplier. The signals were recorded using a digital oscilloscope connected to a computer. All data were taken at room temperature.

III. RESULTS AND DISCUSSION

A. Optical absorption and spectroscopic parameters

The experiments were performed using samples containing different Tm^{3+} and Nd^{3+} concentrations with matrix compositions presented in Table I.

Figure 1 presents the absorption spectra of the samples that display the positions of the Tm^{3+} and Nd^{3+} multiplets located in the energy band gap of the TFP glass. All transitions are inhomogeneously broadened and their bandwidths are larger than the spectrophotometer resolution. The absorption bands represent transitions from the Tm^{3+} ground state ($^3H_6$) and from the Nd^{3+} ground state ($^4I_{9/2}$) to the excited states of the 4f configuration of the respective ion. The spectra of the samples containing Tm^{3+} and Nd^{3+} present all lines shown in Figs. 1(a) and 1(b) for the singly doped samples.

To analyze the results we recall that the majority of the absorption bands in RE ions are associated to electric dipole
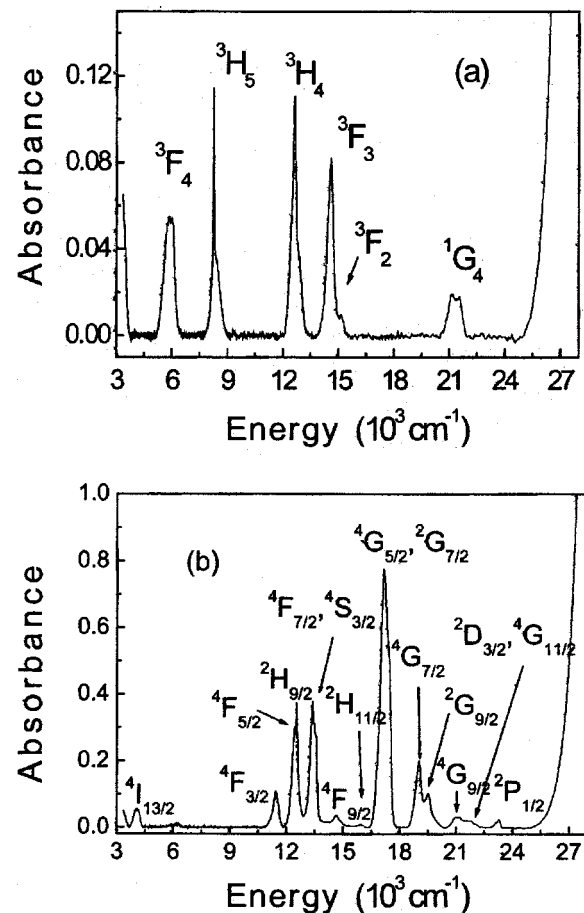

FIG. 1. Absorption spectra of representative samples: (a) NBW(1Tm); (b) NBW(1Nd). Samples thickness: 2 mm.

(ED) transitions but few magnetic dipole (MD) transitions are known. The dipole strength, P, of a transition, written in esu units, can be expressed as[20]

$$P = \frac{mc^2 n^2}{N\pi e^2 \chi_a} \int \kappa(\nu) d\nu, \tag{1}$$

where m is the electron mass, c the speed of the light, N is the number of ions per unit volume, e the electron charge, n is the refractive index of the sample, and $\int \kappa(\nu) d\nu$ is the integrated absorption coefficient which is determined from the absorption spectrum. The Lorentz local field factor for ED transitions is $\chi_a = (n^2+2)^2/9n$. The refractive index, measured using the prism-coupling technique, is 1.70 at 632.8 nm.

The oscillator strength of a transition between two states aJ and bJ' can be calculated using the Judd-Ofelt (JO) theory[20,21] and is given by

$$P = \frac{8\pi^2 mc\bar{\nu}}{3h(2J+1)} \chi_a \sum_{\lambda=2,4,6} \Omega_\lambda |\langle aJ\|U^{(\lambda)}\|bJ'\rangle|^2, \tag{2}$$

where $\bar{\nu}$ is the mean frequency between the two states (in cm^{-1}), $U^{(\lambda)}$ (λ=2,4,6) are tensor operators of rank λ, and Ω_λ are the JO intensity parameters. The terms $\langle aJ\|U^{(\lambda)}\|bJ'\rangle$ are the reduced matrix elements that are host independent. The values used here were obtained from Ref. 22. The Ω_λ

TABLE II. Dipole strengths of Nd^{3+} transitions from $^4I_{9/2}$.

aJ	bJ'	Energy gap (cm^{-1})	P_{exp} ($\times 10^{-6}$)	P_{theo} ($\times 10^{-6}$)
$^4I_{9/2}$	$^4I_{13/2}$	4054	1.32	1.91
	$^4F_{3/2}$	11 440	2.48	2.58
	$^4F_{5/2}, ^2H_{9/2}$	12 469	8.41	8.93
	$^4F_{7/2}, ^4S_{3/2}$	13 416	9.77	9.43
	$^4F_{9/2}$	14 581	1.65	7.14
	$^4G_{5/2}, ^2G_{7/2}$	17 182	2.84	2.84
	$^4G_{7/2}$	19 006	4.99	4.86
	$^2G_{9/2}$	19 533	2.78	1.71

parameters are determined by the standard-least squares fitting method.

Equation (1) allow to calculate P for each transition and these values can be used in Eq. (2) to determine the JO parameters. The spontaneous emission probability between aJ and bJ' states is

$$A_{JJ'} = \frac{64\pi^4}{3h(2J+1)\lambda^3}\left\{\frac{n(n^2+2)^2}{9}S_{ED} + n^3 S_{MD}\right\}. \qquad (3)$$

The ED line strengths is defined as

$$S_{ED} = e^2 \sum_{\lambda=2,4,6} \Omega_\lambda |\langle aJ\|U^{(\lambda)}\|bJ'\rangle|^2, \qquad (4)$$

and the MD line strength is given by

$$S_{MD} = \left(\frac{e^2 h^2}{16\pi^2 m^2 c^2}\right)|\langle aJ\|L+2S\|bJ'\rangle|^2. \qquad (5)$$

S_{ED} is host dependent through the Ω_λ parameters while S_{MD} is independent of the host.

MD transitions can only take place between components of the same LS coupling multiplet for which $\Delta J = 0, \pm 1$. Their dipole strengths assume values that are one order of magnitude smaller than S_{ED}.[2] Therefore, the contribution of S_{MD} will be neglected here.

The radiative lifetime of an excited state is calculated by $\tau_R = (\Sigma_{J'} A_{JJ'})^{-1}$ and the branching ratio corresponding to the emission from level J to J' is given by $\beta_{JJ'} = A_{JJ'}\tau_R$.

Table II presents the dipole strengths obtained for the Nd^{3+} ion using the optical absorption spectrum and Eqs. (1) and (2). The JO parameters calculated were $\Omega_2 = 7.28 \times 10^{-20}$ cm^2, $\Omega_4 = 4.55 \times 10^{-20}$ cm^2, and $\Omega_6 = 6.18 \times 10^{-21}$ cm^2. The root-mean-square deviation of the measured and calculated line strengths was 3.1×10^{-7}. The radiative transition probabilities, the branching ratios for each Nd^{3+} transition and the radiative lifetimes of all levels are presented in Table III. The spectroscopic parameters related to Tm^{3+} were given in Ref. 17. Notice that although the band corresponding to $^3H_6 \rightarrow ^1D_2$ (Tm^{3+}) transition is not observed in the absorption spectrum of Fig. 1, its energy was determined in Ref. 17 performing an experiment where fluorescence in the blue region was investigated exciting the samples in the ultraviolet region. The position of level $^1D_2$ was determined as 28 061 cm^{-1}. The relatively narrow fluorescence bandwidth and the frequency corresponding to the $^1D_2 \rightarrow ^3H_6$ transition show that the overlap between the $4f$

TABLE III. Transitions from $(SL)J$ to $(S'L')J'$ states. Energy gap (ΔE), radiative transition probability ($A_{JJ'}$), Branching ratio ($\beta_{JJ'}$), and radiative lifetime (τ_R) of Nd^{3+}.

$(SL)J$	$(S'L')J'$	ΔE (cm^{-1})	$A_{JJ'}$ (s^{-1})	$\beta_{JJ'}$	τ_R (μs)
$^4I_{11/2}$	$^4I_{9/2}$	2114	18.44	1.000	54 232
$^4I_{13/2}$	$^4I_{11/2}$	1940	13.20	0.244	18 473
	$^4I_{9/2}$	4054	40.94	0.756	
$^4I_{15/2}$	$^4I_{13/2}$	2062	15.84	0.267	16 838
	$^4I_{11/2}$	4002	31.58	0.532	
	$^4I_{9/2}$	6116	11.96	0.201	
$^4F_{3/2}$	$^4I_{15/2}$	5324	19.55	0.005	258
	$^4I_{13/2}$	7386	390.17	0.101	
	$^4I_{11/2}$	9326	1924.98	0.496	
	$^4I_{9/2}$	11 440	1546.81	0.399	
$^4F_{5/2}$	$^4F_{3/2}$	956	0.35	0.000	199
	$^4I_{15/2}$	6280	175.70	0.035	
	$^4I_{13/2}$	8342	957.27	0.190	
	$^4I_{11/2}$	10 282	542.41	0.108	
	$^4I_{9/2}$	12 396	3353.99	0.667	
$^2H_{9/2}$	$^4F_{5/2}$	155	0	0	1145
	$^4F_{3/2}$	1111	0.08	0	
	$^4I_{15/2}$	6435	116.38	0.133	
	$^4I_{13/2}$	8497	195.54	0.224	
	$^4I_{11/2}$	10 437	61.00	0.070	
	$^4I_{9/2}$	12 551	500.26	0.573	
$^4F_{7/2}$	$^2H_{9/2}$	836	0.05	0	191
	$^4F_{5/2}$	991	0.46	0	
	$^4F_{3/2}$	1947	1.13	0	
	$^4I_{15/2}$	7271	649.86	0.124	
	$^4I_{13/2}$	9333	458.55	0.087	
	$^4I_{11/2}$	11 273	1592.00	0.303	
	$^4I_{9/2}$	13 387	2543.80	0.485	
$^4S_{3/2}$	$^4F_{7/2}$	182	0	0	181
	$^2H_{9/2}$	1018	0.02	0	
	$^4F_{5/2}$	1173	0	0	
	$^4F_{3/2}$	2129	0	0	
	$^4I_{15/2}$	7453	5.75	0.001	
	$^4I_{13/2}$	9515	1313.23	0.238	
	$^4I_{11/2}$	11 455	1459.68	0.265	
	$^4I_{9/2}$	13 569	2734.04	0.496	
$^4F_{9/2}$	$^4S_{3/2}$	1012	0.01	0	245
	$^4F_{7/2}$	1194	0.80	0	
	$^2H_{9/2}$	2030	0.95	0	
	$^4F_{5/2}$	2185	3.07	0.001	
	$^4F_{3/2}$	3141	6.59	0.002	
	$^4I_{15/2}$	8465	932.30	0.228	
	$^4I_{13/2}$	10 527	1449.91	0.355	
	$^4I_{11/2}$	12 467	1414.45	0.346	
	$^4I_{9/2}$	14 581	277.82	0.068	

wave functions and the extended Bloch waves of the glass is small. This result is in agreement with Ref. 23 where excited states of Tm^{3+} with energy larger than the energy gap of gallium lanthanum sulfide glasses were shown as efficiently shielded. Similar observations were reported for Tm^{3+} doped fluorophosphate glasses.[9]

B. Infrared emission and blue up-conversion fluorescence

Figure 2 shows the fluorescence spectrum corresponding to Tm^{3+} transitions $^1D_2 \rightarrow ^3F_4$ (centered at $\approx$454 nm) and
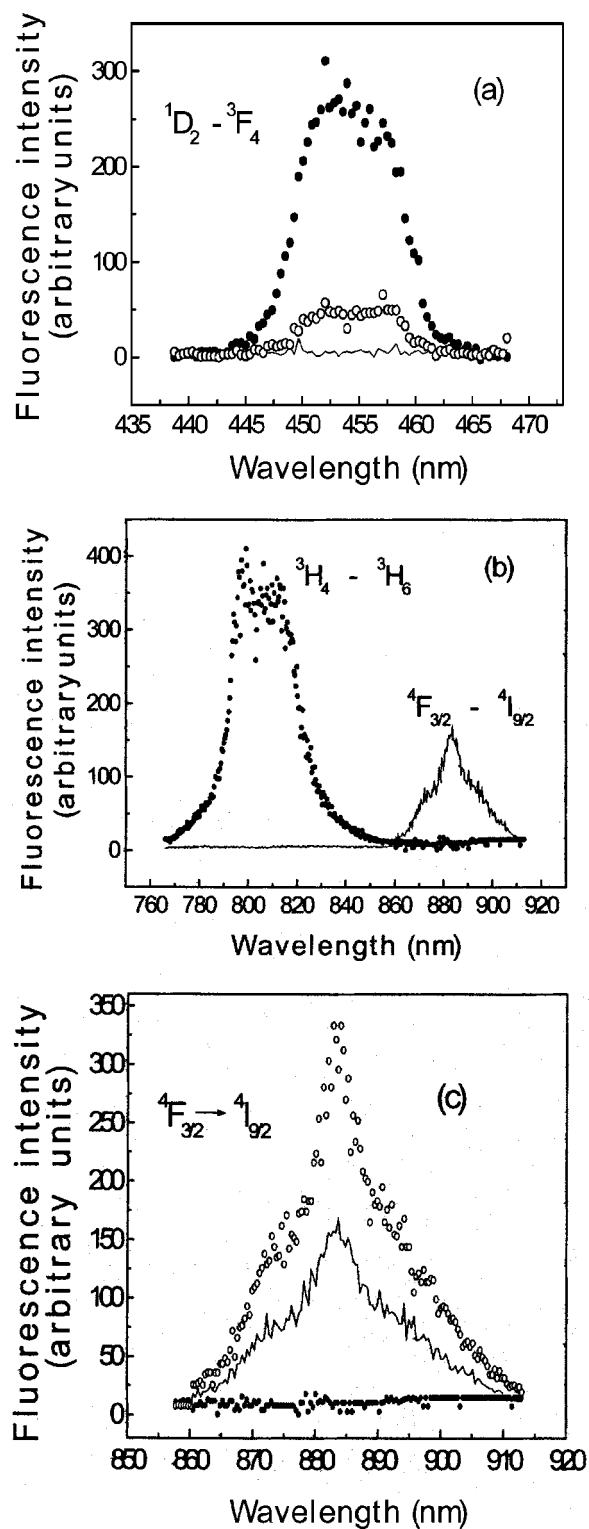
FIG. 2. Fluorescence spectra for excitation at 660 nm. (a) Up-conversion emission $^1D_2 \rightarrow {}^3F_4$ in Tm^{3+}. (b) Infrared emission corresponding to transitions $(^3H_4 \rightarrow {}^3H_6)$ in Tm^{3+} and $(^4F_{3/2} \rightarrow {}^4I_{9/2})$ in Nd^{3+}; (c) change in the $(^4F_{3/2} \rightarrow {}^4I_{9/2})$ signal due to energy transfer from Tm^{3+} [sample NBW(1Tm)—closed circles; sample NBW(1Nd)—solid line; sample NBW(0.2Tm;1Nd)—open circles].

$^3H_4 \rightarrow {}^3H_6$ (centered at ≈ 800 nm), and to Nd^{3+} transition $^4F_{3/2} \rightarrow {}^4I_{9/2}$ (centered at ≈ 880 nm). These results were obtained with the dye laser operating at 660 nm, in resonance with transition $^3H_6 \rightarrow {}^3F_2$. Figure 2(a) shows a linear decrease of the UC emission with Tm^{3+} concentration. Figure

2(b) shows the fluorescence spectrum obtained with samples NBW(1Tm) and NBW(1Nd) from 760 to 910 nm. The measurements show that the emission at ≈ 800 nm is due to the Tm^{3+} ions and the emission at ≈ 880 nm is due to Nd^{3+} ions. Both emissions are also observed in the codoped samples containing Tm^{3+} and Nd^{3+}. Figure 2(c) shows enhancement of the Nd^{3+} emission at ≈ 880 nm due to the presence of Tm^{3+} in the samples. Note that the intensity at ≈ 880 nm increases by $\approx 100\%$ when 0.2% of Tm^{3+} is added to the sample with 1.0% of Nd^{3+}. We recall that level $^4F_{3/2}$ has a long lifetime and is usually exploited for laser emission in various hosts.

The dependence of the fluorescence signals with the laser intensity was investigated for all samples. It was observed that the UC intensity at ≈ 454 nm presents a quadratic dependence as a function of the laser intensity indicating that a two-photon absorption process originates the blue emission. The emission at ≈ 800 nm, corresponding to transition $^3H_4 \rightarrow {}^3H_6$ (Tm^{3+}), is due to the excitation of $^3H_6 \rightarrow {}^3F_3$ transition with subsequent nonradiative relaxation (NRR) to level $^3H_4$ from where the emission at ≈ 800 nm originates. NRR from $^3F_2$ and $^3F_3$ levels to the $^3H_4$ state by multiphonon relaxation (MPR) is efficient because of the relatively small energy gap (≈ 2000 cm^{-1}) which corresponds to less than the energy of three cutoff phonons of the glass matrix.

The signal intensity at ≈ 880 nm presents a linear dependence with the laser intensity indicating that only one laser photon is involved in the excitation process. This emission is enhanced due to ET from Tm^{3+} to Nd^{3+} and the attributed ET pathway is from level $^3H_4$ to $(^2H_{9/2}, {}^4F_{5/2})$ because of the large spectral overlap between these levels and because the oscillator strength of transitions $^4F_{5/2} \rightarrow {}^4I_{9/2}$ and $^3H_4 \rightarrow {}^3H_6$ are both very large. State $^4F_{3/2}$ is populated by NRR from $^4F_{5/2}$ and emission at ≈ 880 nm is observed corresponding to $^4F_{3/2} \rightarrow {}^4I_{9/2}$.

Excitation spectra of the emissions centered at ≈ 454, ≈ 800, and ≈ 880 nm were recorded to investigate further the excitation routes corresponding to the observed fluorescence signals. The results for all samples are similar. Figure 3(a) shows that the blue emission is peaked when the excitation wavelength is ≈ 660 nm corresponding to resonant excitation of transition $^3H_6 \rightarrow {}^3F_2$. This is in agreement with previous observation reported for Tm^{3+} doped TFP,[17] and the emission corresponding to $^1D_2 \rightarrow {}^3F_4$ transition is due to the NRR from $^3F_4$ to $^3H_4$ followed by the excited state absorption $^3H_4 \rightarrow {}^1D_2$. Figures 3(b) and 3(c) show that the other two emissions reaches maximum amplitude when the laser wavelength corresponds to the resonant excitation of the $^3H_6 \rightarrow {}^3F_3$ transition, which is two times more efficient than transition $^3H_6 \rightarrow {}^3F_2$. The absorption of radiation at 657.7 nm is mainly due to Tm^{3+} ions because the oscillator strengths of transition $^4I_{9/2} \rightarrow {}^4F_{9/2}$ in Nd^{3+} is $\approx$ ten times smaller than the oscillator strength of transition $^3H_6 \rightarrow {}^3F_3$.

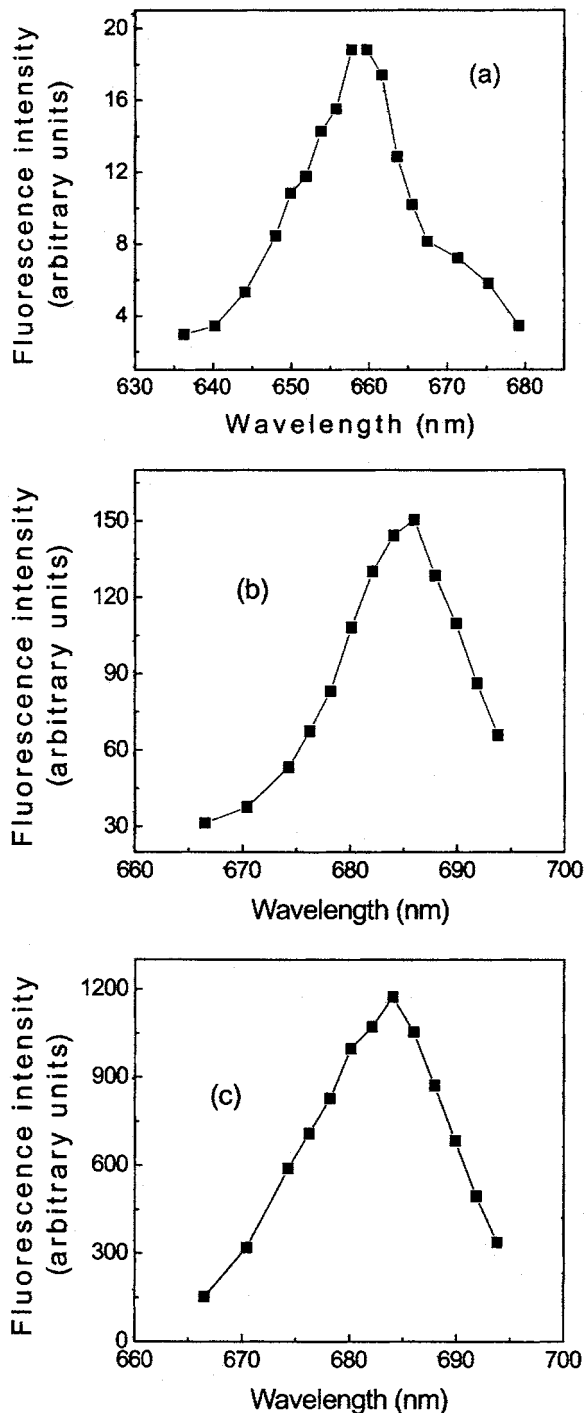Figure 4 summarizes the pathways followed by the excitation energy for the fluorescence signals.

FIG. 3. Excitation spectrum of the blue and infrared emissions [sample: NBW(0.2Tm;1Nd)]: (a) emission at ≈ 454 nm; (b) at ≈ 800 nm; (c) at ≈ 883 nm.
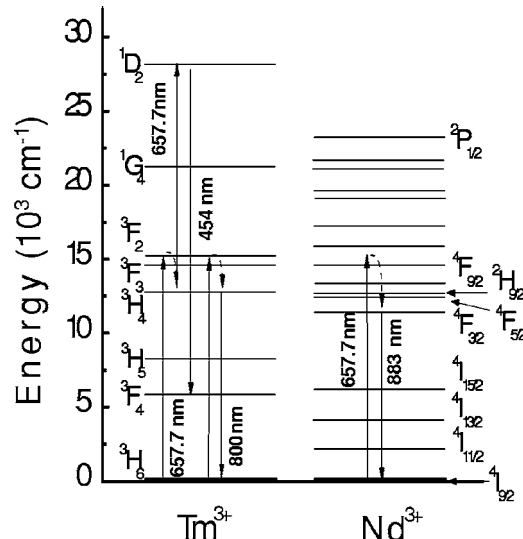

FIG. 4. Energy level diagram of Tm^{3+} and Nd^{3+} ions with indication of the transitions studied. The solid lines represent laser-induced transitions and dashed lines refer to nonradiative transitions.

which includes the MPR rate (W_{MP}) and ET rate (W_{ET}) to neighbor RE ions. The difference between the theoretical and the measured lifetime of the $^3H_4$ level in the sample NBW(0.2Tm) is due to the MPR contribution and its value ($W_{MP}=48\,442$ s^{-1}) was already determined in Ref. 17. The decrease of the $^3H_4$ level lifetime when Nd^{3+} is introduced in the TFP samples is another indication that ET processes are contributing for the relaxation of Tm^{3+} ions. The results in Table IV indicate that W_{NR} increases as the Nd^{3+} concentration is increased which is usual when ET processes are relevant. The lifetimes reported correspond to an average of three measurements but the uncertainty of 1 μs does not allow a precise determination of W_{ET}. Taking into account the value determined for W_{MP} for sample NBW(0.2Tm) and a lifetime of 15 μs it is possible to estimate the order of magnitude of W_{ET} as 1.7×10^4 s^{-1}. This is a reasonable value because the ET process is resonant.

In the case of the $^4F_{3/2}$ (Nd^{3+}) multiplet we first note that the value τ ($^2F_{3/2}$)=203 μs for sample NBW(1Nd) is smaller than the lifetime determined using JO theory that is 258 μs. From this we determine $W_{NR}=1050$ s^{-1}. Since the energy gap between levels $^4F_{3/2}$ and $^4I_{15/2}$ is ≈ 5324 cm^{-1}, a small $W_{MP} \approx 80$ s^{-1} is expected if W_{MP} is estimated using the energy gap law.[2] Hence, an ET rate of 970 s^{-1} is obtained for

C. Excited states lifetimes and energy transfer rates

The lifetimes of states $^3H_4$ (Tm^{3+}) and $^4F_{3/2}$ (Nd^{3+}) were determined and compared with the predictions based on the JO theory. As shown in Table IV the measured lifetimes are different from the calculated radiative lifetimes. This indicates that the contributions of nonradiative processes due to MPR and/or ET have to be considered. Accordingly, the excited state lifetime is given by $\tau^{-1}=\tau_R^{-1}+W_{NR}$, were τ is the actual lifetime, τ_R is the radiative lifetime calculated using the JO theory, and W_{NR} is the nonradiative relaxation rate

TABLE IV. Experimental and theoretical lifetimes of levels $^3H_4$ (Tm^{3+}) and $^4F_{3/2}$ (Nd^{3+}).

Sample	$^3H_4$ (Tm^{3+})	$^4F_{3/2}$ (Nd^{3+})
Theoretical radiative lifetime	640 μs	258 μs
Experimental lifetime		
NBW(0.2Tm)	(20±1) μs	⋯
NBW(0.2Tm;0.5Nd)	(16±1) μs	(183±2) μs
NBW(0.2Tm;0.75Nd)	(15±1) μs	(170±2) μs
NBW(0.2Tm;1Nd)	(13±1) μs	(160±2) μs
NBW(1Nd)	⋯	(203±2) μs

processes involving Nd^{3+} ions. For the sample NBW(0.2Tm;1Nd) a value for $W_{ET}=1324$ s^{-1} can be determined comparing the measured lifetime of $^4F_{3/2}$ level and the result for sample NBW(1Nd). The most probable mechanism of ET in this case is a cross relaxation $[Nd^{3+}(^4F_{3/2}):Tm^{3+}(^3H_6)] \rightarrow [Nd^{3+}(^4I_{15/2}):Tm^{3+}(^3F_4)]$. Accordingly, Table IV indicates that the lifetime of level $^4F_{3/2}$ increases with reduction of the Nd^{3+} content as expected when cross relaxation is present.

IV. CONCLUSION

The results for (Tm^{3+},Nd^{3+}) doped tungstate fluorophosphate glass in this paper can be summarized in the following way: (i) the radiative relaxation rates, the branching ratios, and the fluorescence lifetimes of Nd^{3+} were calculated based upon linear absorption measurements and the Judd-Ofelt theory; (ii) energy transfer rates among Tm^{3+} and Nd^{3+} ions were estimated from the analysis of the temporal behavior of the fluorescence signals; and (iii) the excitation pathways for the frequency up-conversion process and the linear fluorescence observed were identified with basis on the analysis of the experiments.

The data presented here and the previous results of Refs. 16–19, demonstrate the large potential of the TFP glass for photonic applications. A patent was recently deposited[24] where the effect of two-photon absorption in TFP glass was exploited for three-dimensional (3D) optical storage. Presently we are using RE ions-doped TFP samples to develop single-mode fibers and planar waveguides, aiming the investigation of the materials performance as optical amplifiers.

ACKNOWLEDGMENTS

[1]*Rare Earth Doped Fiber Lasers and Amplifiers*, edited by M. J. F. Digonet (Dekker, New York, 1993), and references therein.

[2]See, for instance, M. Yamane and Y. Asahara, *Glasses for Photonics* (Cambridge University Press, Cambridge, UK, 2000), and references therein.

[3]R. S. Quimby, J. Appl. Phys. **90**, 1683 (2001).

[4]W. Tian and B. R. Reddy, Opt. Lett. **26**, 1580 (2001).

[5]For a review on fluoroindate glasses see C. B. de Araújo, G. S. Maciel, L. de S. Menezes, N. Rakov, E. L. Falcão-Filho, V. A. Jerez, and Y. Messaddeq, C. R. Chim. **5**, 885 (2002).

[6]V. A. Jerez, C. B. de Araújo, and Y. Messaddeq, J. Appl. Phys. **96**, 2530 (2004).

[7]S. Kishimoto and K. Hirao, J. Appl. Phys. **80**, 1965 (1996).

[8]I. R. Martin, V. D. Rodrigues, R. Alcala, and R. Cases, J. Non-Cryst. Solids **161**, 294 (1993).

[9]K. Binnemans, R. Van Deun, C. Görler-Walrand, and J. L. Adam, J. Non-Cryst. Solids **238**, 11 (1998).

[10]G. Ozen, A. Kermaoui, J. P. Denis, W. Xu, F. Pelle, and B. Blansat, J. Lumin. **63**, 85 (1995).

[11]A. P. Otto, K. S. Brewer, and A. J. Silversmith, J. Non-Cryst. Solids **265**, 176 (2000).

[12]N. Rakov *et al.*, J. Appl. Phys. **92**, 6337 (2002).

[13]J. Qiu and Y. Kawamoto, J. Fluorine Chem. **110**, 175 (2001).

[14]R. Balda, J. Fernandez, A. de Pablos, J. M. F. de Navarro, and M. A. Arriandiaga, Phys. Rev. B **53**, 5181 (1996).

[15]R. Van Deun, K. Binnemans, C. Görller-Walrand, and J. L. Adam, J. Alloys Compd. **283**, 59 (1999).

[16]G. Poirier, M. Poulain, Y. Messaddeq, and S. J. L. Ribeiro, J. Non-Cryst. Solids **351**, 293 (2003).

[17]G. Poirier, V. A. Jerez, C. B. de Araújo, Y. Messaddeq, S. J. L. Ribeiro, and M. Poulain, J. Appl. Phys. **93**, 1493 (2003).

[18]G. Poirier, C. B. de Araújo, Y. Messaddeq, S. J. L. Ribeiro, and M. Poulain, J. Appl. Phys. **91**, 10221 (2002).

[19]E. L. Falcão-Filho, C. B. de Araújo, C. A. C. Bosco, L. H. Acioli, G. Poirier, Y. Messaddeq, G. Boudebs, and M. Poulain, J. Appl. Phys. **96**, 2525 (2004).

[20]B. R. Judd, Phys. Rev. **127**, 750 (1962).

[21]G. S. Ofelt, J. Chem. Phys. **37**, 511 (1962).

[22]W. T. Carnall, H. Crosswhite, and H. M. Crosswhite, *Energy Level Structure and Transition Probabilities of Trivalent Lanthanides in LaF$_3$* (Argonne National Laboratory Report, Illinois, 1977).

[23]T. Schweizer, P. E. A. Möbert, J. R. Hector, D. W. Hewak, W. S. Brocklesby, D. N. Payne, and G. Huber, Phys. Rev. Lett. **80**, 1537 (1998).

[24]G. Poirier, M. Nalin, Y. Messaddeq, and S. J. L. Ribeiro, Patent No. PI 0502711 (pending).